UNITED NATIONS UNIVERSITY
UNU-GTP
Geothermal Training Programme

Orkustofnun, Grensasvegur 9,
IS-108 Reykjavik, Iceland

Reports 2016
Number 27

COGENERATION OF POWER AND HEAT IN HUNGARY

Anna Medgyesy
41. Szolo Street
Budajeno
HUNGARY
medgyesy.anna@gmail.com

ABSTRACT

For the first time in Hungary, a geothermal ORC power plant is being built, and will have the capacity to generate 2.2-2.5 MW of electricity. It is located in Tura, 30 km east of Budapest. After a long design and optimisation procedure, some questions are still unanswered. This paper reports answer to some of these, like how much heat the power plant can provide for the greenhouse designed near to the power plant, and how much water is needed to replace the evaporated water in the evaporative condenser, as well as how the ambient temperature will influence the screw expanders power output through the condenser. To evaluate these tasks, a Scilab code was written. The main parameters were provided by Mannvit Consulting Engineers.

1. INTRODUCTION

Hungary is a country with a good low-temperature geothermal potential, suitable for direct use, such as district heating or bathing. Recently, new possibilities have opened up, as in Tura, 30 km east of Budapest, where Hungary's first geothermal electric power plant is being built, or in Dombóvár, where plans have also been proposed for electricity production (Unyi, 2016).

Tura is a small town and the site of first ORC power plant to be built in Hungary. The power plant is scheduled to generate up to 2.5 MW of electricity to the network. Commissioning the power plant has an added value, not just because it will raise the share of renewables in electricity generation, but it will also serve as good practice, and give new knowledge to Hungary. This report presents a hypothetical investigation of a planned Organic Rankine Cycle power plant in Hungary. The main task was to determine the needed heat supply for an 11-ha. greenhouse complex intended for tomato growing, with the geothermal water provided by the power plant. Additional task was to assess the net power output of the power plant versus ambient temperatures. The ambient temperature influences the greenhouse heat requirements as well as the working efficiency of the planned evaporative condenser. Many parameters are unknown here, like the exact design of the greenhouse, or the mass flow and pressure ratio of the ORC fluid in the power plant, hence this discussion must be looked at as hypothetical.

The ORC plant has two loops, a high-temperature one and a low-temperature one, a total nominal rated output at generator of 3350 kW and design gross power of 2619 kW. The geothermal fluid mass flow is 86 kg/s, the inlet temperature 124°C. When the plant is operating only 45 kg/s are available at 78°C, flowing to the greenhouse. The plant investment cost based on the latest news is around 10 billion HUF (circa 3,225,000 EUR), 5.5 billion HUF is expected to cover the capital cost of the ORC plant, the rest will be spent on the greenhouse complex, which is designed to cover 11 ha. (Magyar Idők, 2016; Alternatív Energia, 2016). The project will be financed by foreign investors, EU assistance, bank loans and Hungarian investors. To know the possible heat supply, and the temperature effect on the power output can be crucial in the ROI (Return On Investiment) calculations. Scilab free software was used for the calculation, with Coolprop fluid properties extension. Scilab is more or less similar to Matlab and CoolProp is similar to REFPROP (Scilab, 2016; CoolProp, 2016; MATLAB, 2016; REFPROP, 2016).

This project was carried out as the final project of the author's six-month geothermal training in Iceland at the United Nations University Geothermal Training Programme (UNU-GTP). The main project objectives were the following:

- How much income can the scheduled Tura power plant possibly have from selling heat to an 11-ha. tomato greenhouse complex?
- How much water evaporates in the evaporative condenser as a function of the ambient temperature?
- How will ambient temperature through the condenser influence power output of the power plant?

2. PRESTUDY

2.1 The greenhouse

Before determining the energy requirements of the greenhouse complex, Mr. Keszthelyi Krisztián, Department Engineer at Faculty of Economics and Social Sciences, Szent István University, was contacted to gain information on mainstream greenhouse design in Hungary. He provided a lot of useful information, which can influence decisions, and an important part of the model, including the following: During the winter season, there is no tomato production in greenhouses in Hungary, as the Spanish and Jordanian farms control the market, with their cheap prices. They have a competitive advantage, based on their warmer and less radical weather conditions. However, in the winter period Hungarian greenhouses need heat to avoid freezing damage. Using light is not common, as the electricity price is quite high compared to the heat price, and during the greenhouse heating period this is not necessary, as the number of sunny hours is efficient for growing plants inside. Nowadays, typical greenhouses are of Venlo type, with 5×8 m^2 blocks, 22° roof angle, 7.5 m total height, and 4 mm glass layer on the roof and two glass layers on the sides, which can be more than 100 meter long. In Hódmezővásárhely, the new greenhouses, based on measurement made through the Google Earth ruler function, are of the size 140×78 m^2, a size which consequently was used in this project (Google Earth, 2016). It is common to use energy curtains to reduce the heat loss during the night. From practical experience, 20-70% of the heat loss can be reduced by the curtain during night (Sanford, 2011). The tomato plants' optimal growth is depending of course on the species, and the greenhouses are usually operated with daytime temperature of 20-27°C and night-time temperature of 16-18°C (Mariani et al., 2016).

2.2 Energy prices

Some energy prices in Hungary are regulated by law. The renewable energy investment costs can be higher than those for regular natural gas, coal fired or nuclear power plants, depending on the circumstances. This applies especially to places where potential is not high, the renewable energy is seasonable, etc. (OECD, 2015). To enforce the growth of renewable energy against their relative high capital cost, in the European Union there is a common practice, called a *Feed in Tariff*. It is arguable, whether it is a good or bad practice, but it is to be expected that anybody tries to label/emphasize health, environment and risk tax after spreading carcinogenic and health damaging pollutants or causing global warming etc., as the nuclear, natural gas or coal industry, which has a serious effect, not like the CO_2 quota. Life is not just about money and profitability.

Cutting this discussion short, the main point is to make sure the investment will be paid back, support non-government renewable energy investments (independent companies), and ensure that the renewable energy is not lost, and will be used right away in the net, which means almost unlimited access to the network. The renewable electricity prices are presented in Figure 1.

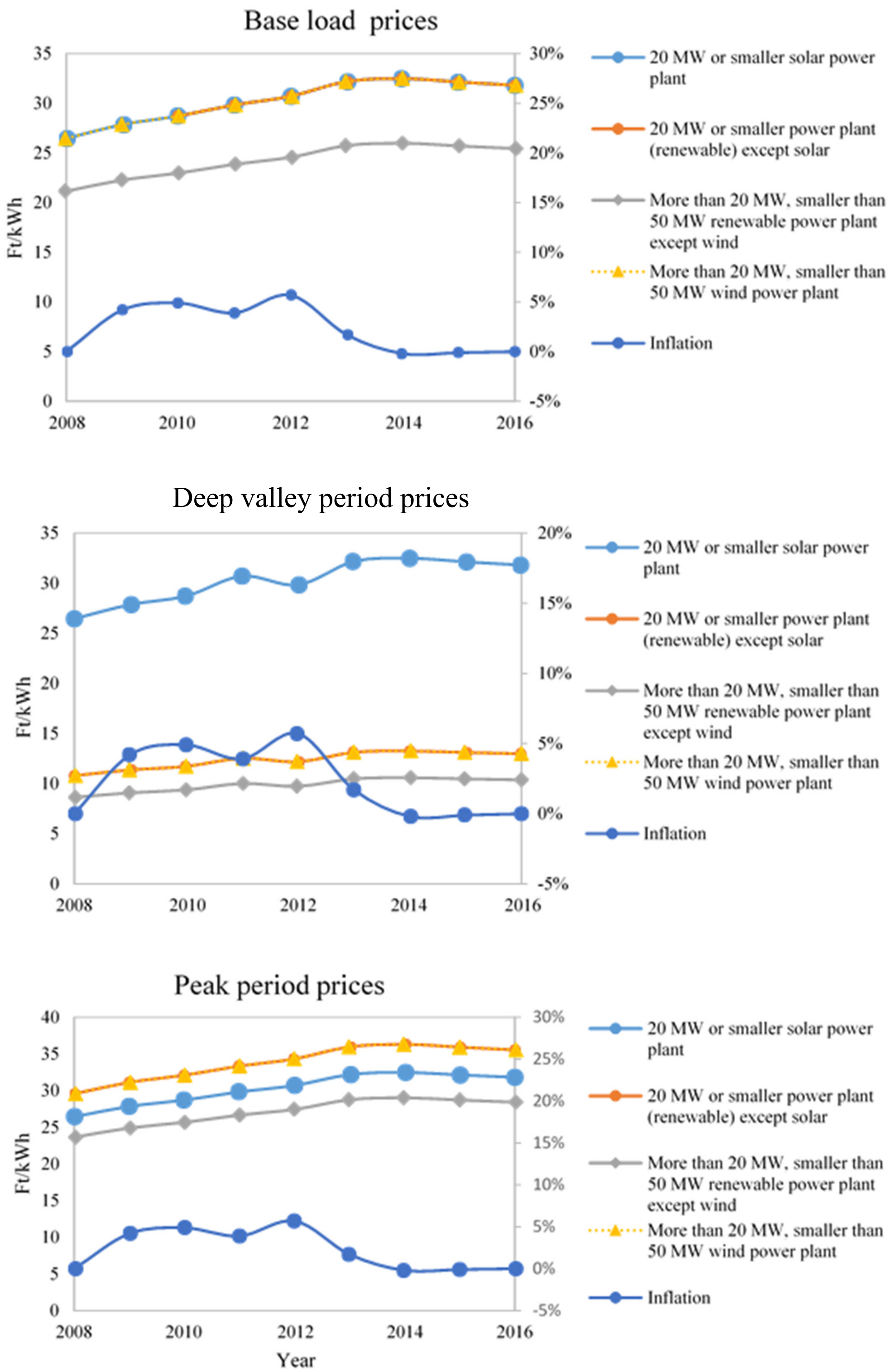

FIGURE 1: Renewable electricity prices

In Hungary district heating is also getting government support, through a regulation intended for regulating the heat price of power plants (Hungarian Ministry of National Development, 2011). District heating is not popular in Hungary, and one of the reasons can be seen in Figure 2. It shows that the sales heating fee is regulated by the government, fixed by the *Regulation of district heating sale fees*. If somebody has his own natural gas boiler, for a non-household consumer with more than 20 m^3/h consumption, the average gas price is between 2540 and 2670 Ft/MJ +VAT (Fögaz, 2016). In all, 69% of the district heating fees are higher than the natural gas fee (and this was even higher before, as the regulation aims to reduce the profits of the companies). This resulted in people leaving the district heating systems in the past.

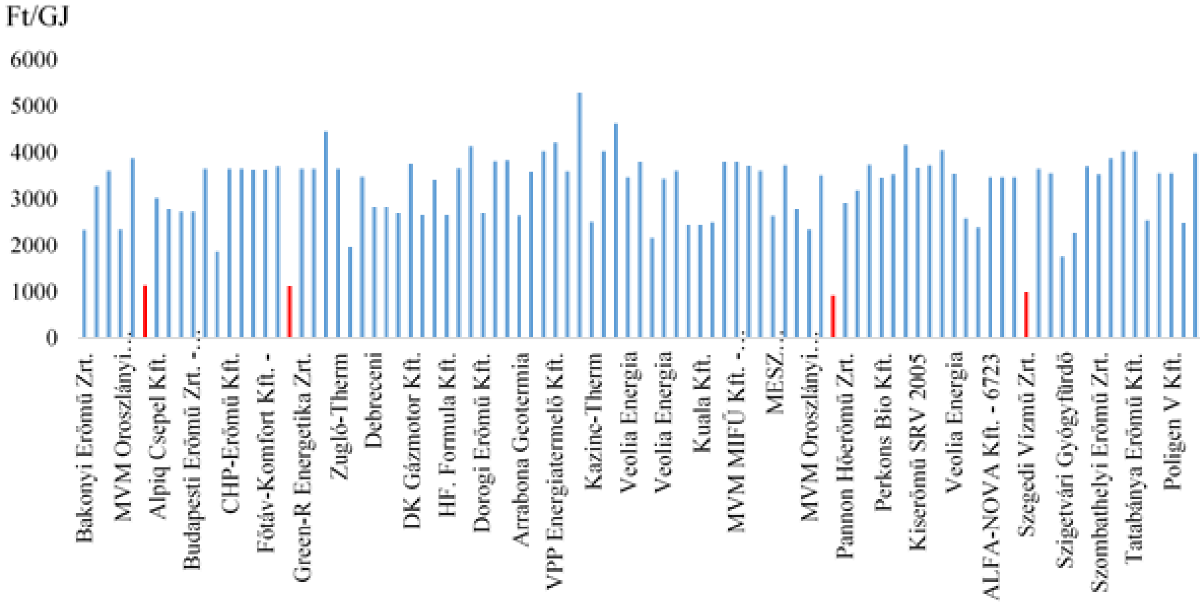

FIGURE 2: District heating suppliers' fixed rate by law

Figure 3 shows non-household consumer gas prices from 1992. It illustrates very well the effect of the economic crisis in 2008. After 2011 the government started to regulate the energy prices to minimise the cost of the households as much as possible. To summarize, the natural gas price in Hungary does not always follow the market trend, but what the politicians want to achieve, and then it depends of course also mostly on the price of Russian natural gas and the contract between the two nations.

In my opinion, in future the natural gas' market price could decrease, as the frozen Siberian gas will be available, and has to be utilised. The renewable energy share is also growing in Europe. In wealthier and environmentally cautious countries, ground source heat pumps may replace the conventional heating systems eliminating the need for the Russian or Dutch natural gas in Europe, which could cause surplus in the system and reduce the prices. The future is unpredictable, everything can happen, the prices can go up or down because of embargo, war, economic crisis, political change, etc. From a capitalist's point of view, if somebody plans a commercial greenhouse and competes on the free market with tomatoes, he/she would choose the cheap natural gas, if the prognosis of the gas price appears cheap in the long term. Consequently, the power plant cannot sell at a higher price than the price would be for laying down the gas pipes (similar as for geothermal water utilisation), paying the fee for the storage capacity, and the fee of the used gas. Comparison of the electricity and gas price gives (Fögaz, 2016):

- *17 Ft/kWh_e* on the electricity market;
- *25-37 Ft/kWh_e* renewable *feed in tariff* (peak, baseload, valley);
- *9.18-9.61 Ft/kWh_{th}* natural gas price.

The decree online about the Tura project (Tura organic garden, 2015) makes it clear that it was prepared to get the *feed in tariff*. From these prices, it can be seen, that the power plant will focus on electricity

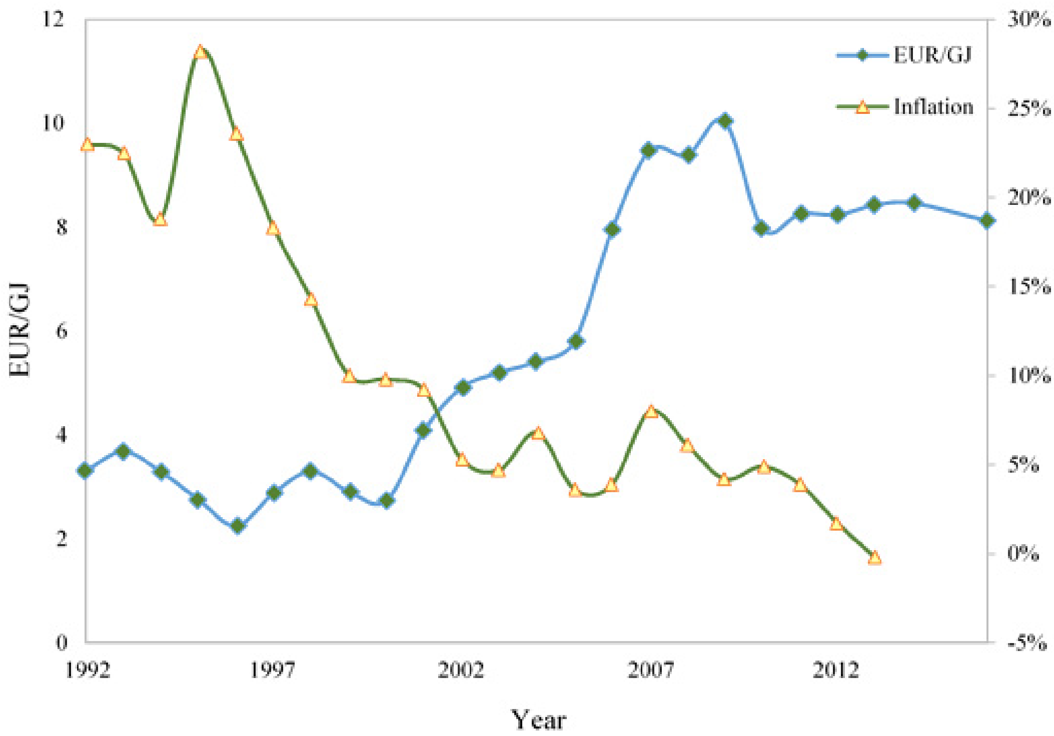

FIGURE 3: Non-household consumer's gas price in Hungary

production, even if the gas price / heat price will be 150-200% higher (for the combined heat and electricity production). It can also be assumed the power plant has to sell the energy at a price close to the actual gas price or lower to be a good choice for the greenhouse owner, unless the greenhouse owner is really environmentally aware or is able to sell the tomatoes with some "green design", which could cover the additional expense.

3. GREENHOUSE HEAT REQUIREMENTS AND GEOTHERMAL HEAT SUPPLY

To estimate the heat requirements of the greenhouse a dynamic model was using Scilab software. The geothermal water inlet mass flow and temperature were the only fixed parameters.

The necessary heat requirements in a greenhouse depend on many factors. There are heat losses by transmission, filtration and ventilation, radiation and vegetable transpiration, evaporation, and water condensation on the surfaces. Heat is gained by solar radiation, and when necessary by the heating system in the greenhouse. I chose to build up a simple model, which doesn't take into account the transpiration and condensation losses but the rest is evaluated. Some assumptions had to be made, including:

- The walls and roof are from glass, the heat transmission across the aluminium frame wasn´t taken into account.
- The temperature control system is PID controlled, mass flow is regulated with a fixed inlet temperature in the radiator, depending on the heat requirement.
- It is presumed that the greenhouse owner is planning to utilise the geothermal heat and the design of the heating system is adapted to this idea. To do that, the design inlet/outlet temperature of the radiator system has to be sufficiently low, not the 90/70°C system, conventional in Hungary. This requires a higher heat exchanger area, which makes it more practical to utilise the geothermal energy, as more energy can be transferred with the same mass flow. A good example can be found

in Iceland, where district heating systems are conventionally run at 80/40°C, successfully for at least 30 years. One of the key factor in the success, is that they use higher heat exchanger surfaces, based on 40°C temperature change in the system, which enables them to utilize twice as much energy, as with the Hungarian 90/70°C forward/return based systems.

- If the geothermal system cannot cover the necessary heat through the heat exchanger, a peak boiler will raise the temperature to the designed water temperature.
- Transpiration of the plants was not considered.
- An 11-ha. greenhouse complex is to be built up from 10 different 140×78.5 m^2 greenhouse blocks.
- Radiation loss was only considered for the roof. It was assumed that all solar radiation is absorbed as heat, which is not reflected by the ground, air or the wall of the greenhouse.
- Air temperature by an ideal ventilator is mixed and uniform everywhere, resulting in no delay in sensing temperature changes.
- If the air temperature exceeds 28°C, the greenhouse roof windows must open, with 28°C being kept preventing the employees suffering from higher temperatures.
- The price of the geothermal heat is assumed to be the same as for natural gas in the income calculation.

Definitions of variables are found in Nomenclature at the end of the report.

For stable conditions, the sum of the heat gain and loss should be zero, as shown in Equation 1:

$$Q_{sr} + Q_{add} - Q_f - Q_t - Q_r = 0 \tag{1}$$

Transmission heat loss from the greenhouse is calculated with Equation 2, where the temperature difference is between the inside temperature in the greenhouse and the outdoor ambient air temperature based on Equation 3. The *U* value was calculated separately for the wall, roof and the ground:

$$Q_t = U \cdot A \cdot \Delta T \tag{2}$$

$$\Delta T = T_{in} - T_{out} \tag{3}$$

The U value in Equation 2 is dependent on the air/ground temperature, the pressure and the velocity of the fluid, in the boundary layers and outside of it. Many theoretical formulae exist for these calculations. In this paper, Equation 4 was used, where δ is the thickness of the wall layer, λ is the conduction heat transfer coefficient of the wall material, and α is the convection heat transfer coefficient of the two sides of the surface. The convective heat transfer coefficient calculations based on the Nusselt number - Reynold number are applicable to liquids, but in the case of gas, often these do not give correct results. Empirical numbers exist for the overall heat transfer coefficient for the greenhouses, with many authors using Rafferty (1998). To the given data a polynomial curve can be fitted and used to estimate the overall heat transfer coefficient in different wind speeds. From the zero wind speed value, the inside convective heat transfer can be calculated from the glass convective heat transfer coefficient. With knowledge on that base value, the roof outside temperature can be determined to estimate the radiative heat loss:

$$U(v_{wind}) = \frac{1}{\frac{1}{\alpha_{in}} + \frac{\delta}{\lambda} + \frac{1}{\alpha_{out}}} \tag{4}$$

The air heat convective heat transfer coefficient is calculated from Equations 5-6:

$$\mathrm{U} = -0.017 * {v_{wind}}^2 + 0.3877 * v_{wind} + 4.4635 \tag{5}$$

$$\alpha_{in} = \frac{2}{\frac{1}{Uo} - \frac{\delta}{\lambda}}, \quad Uo \text{ is evaluated at } v_{wind} = 0 \tag{6}$$

The filtration heat loss is calculated by Equation 7. The heat exchange rate for modern glasshouses is usually $1/h$, but it can change due the ventilation duty, to remove the moisture, avoiding mould and fungus:

$$Q_f = n \cdot c_{p,air} \cdot \rho_{air} \cdot \mathrm{V} \cdot \Delta T \tag{7}$$

The radiation heat loss is calculated by Equations 8-9:

$$Q_r = \delta \cdot \varepsilon_{glass} \cdot A \cdot \mathrm{F} \cdot ({T_{roof,out}}^4 - {T_{sky}}^4) \tag{8}$$

$$T_{roof,out} = T_{out} + \frac{U \cdot A_{roof} \cdot \Delta T}{\alpha_{out}} \tag{9}$$

where the sky temperature is dependent on the opaque cloudiness (and results in lower radiation loss).

The glass temperature can be calculated by the conduction heat transfer coefficient (Equation 9). The sky temperature can be calculated by using Equations 10-12, where *C*, the opaque sky factor (range between 0 and 1), is recorded, usually in historical temperature databases:

$$CF = 1 + 0.00224 \cdot C + 0.0035 \cdot C^2 + 0.0028 \cdot C^3 \tag{10}$$

$$T_{\mathrm{sky}} = T_{\mathrm{amb}} \cdot {\varepsilon_{sky}}^{0.25} \cdot CF^{0.25} \text{ (MW)} \tag{11}$$

$$\varepsilon_{sky} = 0.711 + 0.56 \cdot \frac{T_{\mathrm{air,dew}}}{100} + 0.73 * \frac{T_{\mathrm{air,dew}}}{100}^2 \tag{12}$$

The solar radiation heat gain across a surface is given by Equations 13-20, based on the studies of Zelzouli et al. (2012) and Duffie and Beckman (2013):

$$Q_{sr} = A \cdot (I_{direct} + I_{diffuse,sky} + I_{diffuse,ground}) \tag{13}$$

$$\begin{aligned}\cos\theta = {} & \sin\delta \cdot \sin\varphi \cdot \cos\beta - \sin\delta \cdot \sin\beta \cdot \cos\varphi \cdot \cos\gamma + \cos\delta \cdot \cos\varphi \cdot \cos\beta \\ & \cdot \cos \mathrm{w} + \cos\delta \cdot \sin\varphi \cdot \sin\beta \\ & \cdot \cos\gamma \cdot \cos \mathrm{w} + \cos\delta \cdot \sin\beta \cdot \sin\gamma \cdot \sin \mathrm{w}\end{aligned} \tag{14}$$

$$w = 15(time - 12) \tag{15}$$

$$\delta = 23.45 * \sin\left(\frac{284 + n}{365}\right) \;;\; n \textit{ is the day of the year} \tag{16}$$

$$A = I_{direct}/(I_{global}) \tag{17}$$

$$fm = \left(\frac{I_{direct}}{I_{direct} + I_{diff}}\right)^2 \tag{18}$$

$$\cos\theta_z = \cos\varphi * \cos\delta * \cos \mathrm{w} + \sin\delta \cdot \sin\varphi \tag{19}$$

$$\begin{aligned}I_s = {} & I_{direct} * (1 - r) + I_{diff} * A_s \frac{\cos\theta}{\cos\theta_z} + I_{diff} * (1 - A) * \frac{(1 + \cos\beta)}{2} * (1 \\ & + fm * \sin\frac{\beta}{2})^3 + \left(I_{direct}(1 - r) + I_{diff}\right) * \rho_{ground} \\ & * \frac{(1 - \cos\beta)}{2}\end{aligned} \tag{20}$$

The radiator system is unknown, so was assumed, that an effort will be made to try to fit it to the geothermal heat source and work at design temperatures 73/35 (as the geothermal water is 78°C). It is better not to have direct geothermal flow in the pipe system, as the geothermal fluid in Hungary contains a lot of minerals, and to avoid precipitation the pressure should be kept above 9 bar, which results in higher cost, if the whole system would be designed at 9 bar. The *U* value in the radiator system is not stable at changes with regards to duty and the temperature range. Equation 21 represents an empirical formula, which avoids the use of numerical simulation to determine the pipeline thermodynamic properties in different mass flow and temperatures conditions (Anon 1977), but instead determines the log-mean temperature difference without knowing the exact *U* value in different conditions, where $Q_{0,GH}$ is the design condition:

$$\frac{Q_{GH}}{Q_{0,GH}} = \left(\frac{\Delta Tlg}{\Delta Tlg_0}\right)^{4/3} \tag{21}$$

Through optimization it is decided which case would require a higher built-in capacity, the winter season when the temperature is rarely below -15°C, and a minimum inside temperature of 5°C needs to be kept to avoid freezing, or the autumn/spring season when the minimum temperature is -5°C as a design condition and the heat should be 22°C without radiation heat gain. In different heat duties, a different temperature difference is necessary and different mass flow. Equation 21 determines the necessary temperature difference between the radiator inlet and outlet temperatures and the room-required temperature, and with a basic iteration, the unknown radiator outlet temperature can be defined. By Equation 22 the necessary mass flow can be determined:

$$Q_{GH} = m_{rad} * c_p * (T_{in} - T_{out}) \tag{22}$$

The geothermal heat exchangers traditionally used in Hungary are shell and tube heat exchangers, as the more compact flat-plate collectors can have a high pressure drop and it could cause massive deposition, with the water usually having high mineral content. Here it is assumed, that the pinch point in the heat exchanger is 5°C, and the pinch point is between the lowest radiator return temperature at maximum radiator flow capacity. For that condition, a design *UA* value can be calculated by Equation 23:

$$Q_{HX} = UA * \Delta Tlg_{HX} \tag{23}$$

At a fixed geothermal mass flow and inlet temperature, the most important factor is the geothermal outlet temperature in the heat exchanger in off-design conditions. The outlet temperature of water from the heat exchanger, circulated in the radiators, is also an unknown parameter. The unknown temperatures were determined by Equations 24-25:

$$\Delta Tlg_{HX} = \frac{(T_{g,in} - T_{rad,x}) - (T_{g,out} - T_{rad,return})}{\ln(\frac{T_{g,in} - T_{rad,x}}{T_{g,out} - T_{rad,return}})} \tag{24}$$

$$m_{rad}\left(T_{rad,x} - T_{rad,return}\right)c_p = m_g\left(T_{g,in} - T_{g,out}\right)c_p \tag{25}$$

Different functions were written in Scilab to determine all necessary parameters. The model inlet parameters were the recorded temperature data (EnergyPlus, 2016), an excel sheet containing the year recorded, hourly measured temperatures, relative humidity, wind speed, cloudiness, direct and diffuse solar radiation. The control model used, was a PID mass flow control based on the temperature difference between the reference temperature and the actual temperature, during winter period (T_{ref} = 5°C) and the summer period (from March till November), where the reference temperature was set to 16°C in night and 22°C in day mode, and the day mode was between 6 AM and 6 PM.

4. RESULTS AND DISCUSSION OF THE GREENHOUSE HEAT REQUIREMENTS

The greenhouses were evaluated separately first and the heat losses and gain were calculated, with the necessary mass flow and temperature change for each greenhouse. After some runs it was clear that no significant heat loss or temperature change can be detected if the greenhouses were handled separately. Consequently, this simplification was made and also their heat loss and solar gain handled in the same way, which reduced greatly the time of the calculation runs. Figure 4 shows the heating need of the 11-ha. greenhouse complex per hour for a winter day (January 3rd) without using energy curtains.

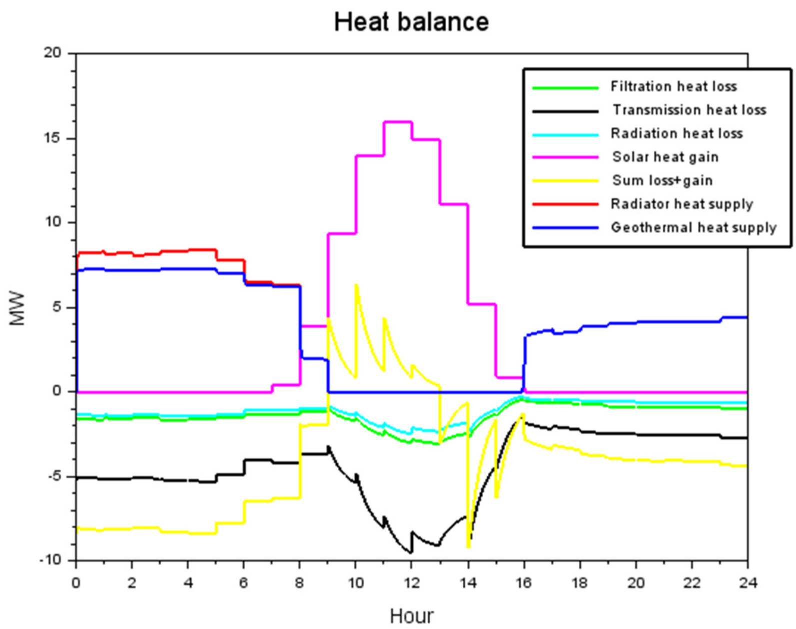

FIGURE 4: Simulation results for heat losses on January 3rd

Even though a dynamic model was made, the data used is not smooth enough, which results in big and sudden step changes in the heat losses, and also in the dynamic response of the system. Transmission and filtration heat loss is dependent on the actual temperature inside, which changes less rapidly than the outlet temperature or wind speed, as can be seen in Figure 5 based on the thermal heat storage effect. Figure 5 represents the influencing parameters of the dynamic model, like the minimum reference temperature, which in the winter season was set to be 5°C, the outlet ambient temperature and the wind speed.

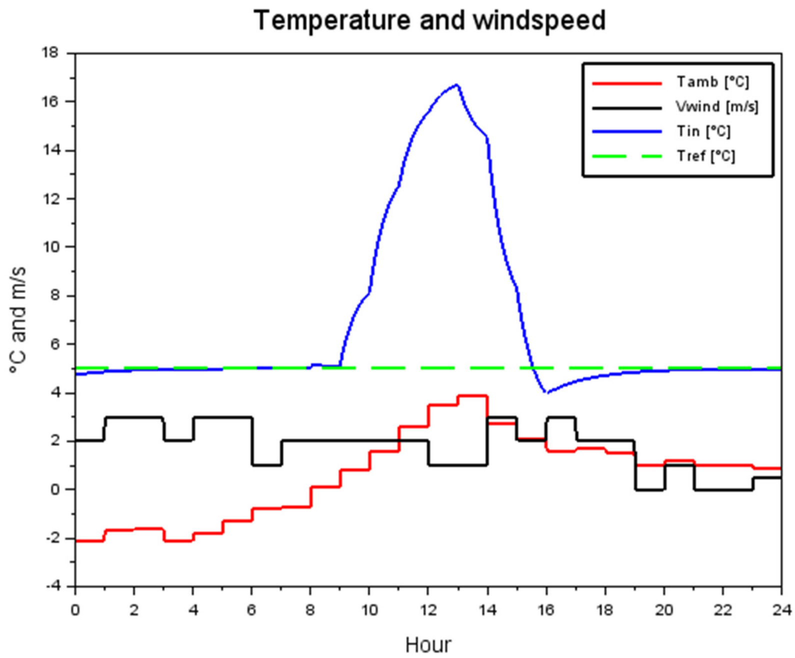

FIGURE 5: Simulation results for influencing factors on January 3rd

Due to the solar radiation and the heat stored in the greenhouse, the inside temperature of the greenhouse rises above the reference temperature. Because of this phenomenon, no additional heat was needed between 8 AM and 4 PM. Figures 6 and 7 show similar simulations for the April 20th heat parameters. The sharp (red) radiator heat supply is due to the change in the reference temperature, and is to warm up the greenhouse. Two different runs were made. In the first case, the heat loss was calculated without the energy curtain and its decreasing heat loss influence. For the other one, the energy curtain was assumed to decrease the heat loss by 45% during the nights. The total supplied energy by the ORC power plant in the first case is 92,436 GJ during a year. If the energy curtain was used, this value was reduced to 65,850 GJ, a decrease of almost 30%. For current

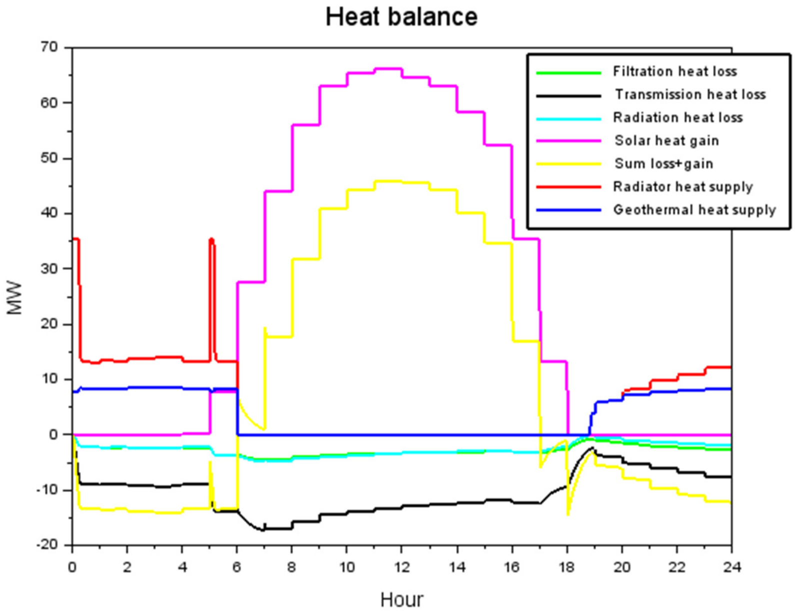

natural gas prices this would mean 250 million HUF (805,000 EUR) in the first case and 178 million HUF (573,500 EUR) in the second case.

FIGURE 6: Simulation results for heat losses on April 20th

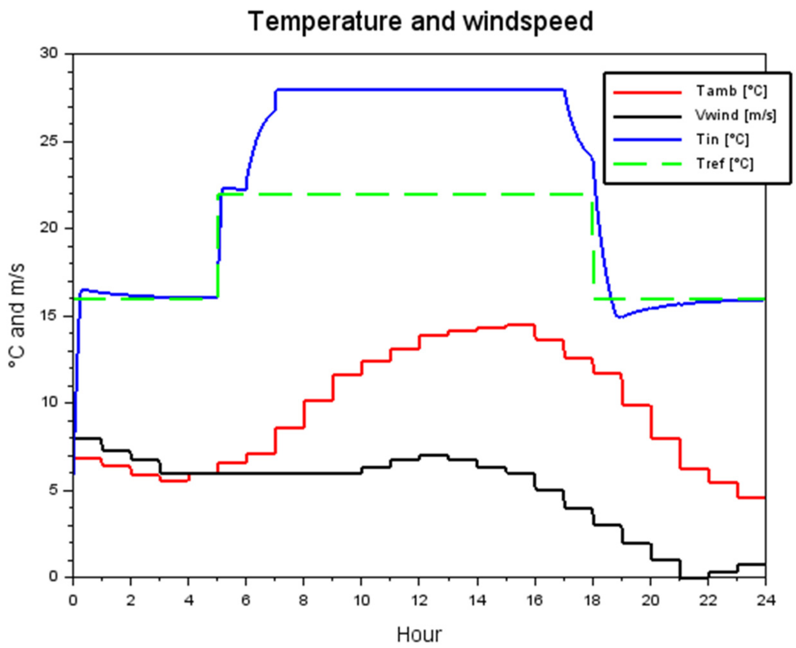

FIGURE 7: Simulation results for influencing factors on April 20th

5. EVAPORATIVE CONDENSER AND POWER OUTPUT

The evaporative condenser is somewhat different from a conventional one because the heat and mass transfer are happening at the same time (Equations 26-27). The condensate gives its heat through the pipe wall to the deluge water, by convection and conduction. The deluge water by conduction and evaporation gives the heat to the airflow (Equations 28-32). Detlev G. Kröger gave a brief description on the process in his book *Air cooled heat exchangers and cooling towers* (Kröger, 2004). Figure 8 shows an elementary control volume and the heat and mass transport in it. The principle of the evaporative condenser is the cooling effect of the water evaporation to the air stream and the high (-er)

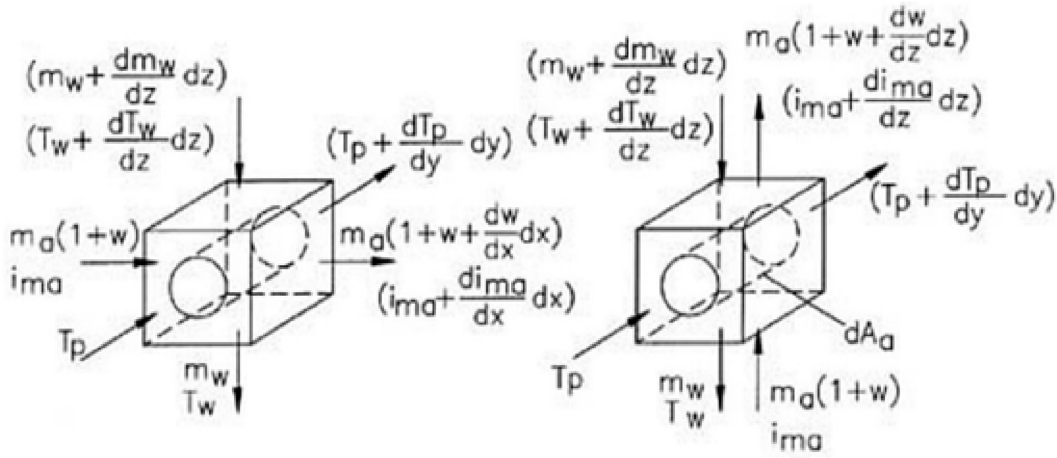

FIGURE 8: Evaporative condenser‘s heat and mass flows (Kröger, 2004)

conductive heat transfer coefficient at the wall-water surface. The driving force of the evaporation is the difference between the air absolute humidity and the air humidity at the water surface (which is assumed to have 100% relative humidity) and the water surface. The basic equations of the evaporative condenser can be found in Kröger’s book and in a thesis by Johan Heyns (Heyns, 2008), but here only the final equations are presented, neglecting the derivation of the formulae which are given in the book or paper.

Some assumptions were made:

- The evaporated water flow compared to the deluge water (circulating) or air mass flow is 10 times smaller, the water flow change can be neglected (but not the evaporation itself);
- The temperature of the water is the same through the tube bundles;
- The air properties values used are the average between the inlet and outlet; and
- The air mass flow is saturated with water at the outlet.

The final simplified case is, that through the whole heat exchanger, the total heat coming from cooling down the ORC fluid and condense it, is equal to the heat transfer through the pipeline given to the deluge water. It is also equal to the heat necessary for evaporation and also the heat transfer from the water to the air. The last two processes mentioned can be expressed as the airstream enthalpy change. The evaporation rate is represented in Equation 29 and the related energy transport by Equation 30. The conductive heat transport is determined by Equation 31.

The equations referred to above are the following:

$$m_{air}(1+w) + \left(m_w + \frac{dm_w}{dz}dz\right) = m_{air}\left[1 + (w + \frac{dw}{dz}dz)\right] + m_w \tag{26}$$

$$m_{air}h_{air} + \left(m_w + \frac{dm_w}{dz}dz\right)(h_w + dh_w) = m_a\left[h_{air} + \frac{dh_{air}}{dz}dz)\right] + m_w h_w \tag{27}$$

$$dQ_{cond\ (ORC\ fluid\ side)} = dQ_{mass} + dQ_{conductive} = Q_{heat+mass\ transfer\ (air\ side)} \tag{28}$$

$$\frac{dm_w}{dz}dz = h_d(w_{ws} - w) * dA \tag{29}$$

$$dQ_{mass} = h_v \frac{dm_w}{dz}dz = h_v h_d (w_{ws} - w) * dA \tag{30}$$

$$dQ_{conductive} = \alpha_a (T_w - T_a) dA \tag{31}$$

$$
\begin{aligned}
Q_{cond} &= m_{R245fa} \cdot \left(\Delta L_{cond} + \Delta h_{R245fa,cool}\right) \\
&= Q_{heat\,transfer} = UA_{bundles}(T_c - T_{wm}) \\
&= Q_{heat+mass\,transfer} = m_{air} \cdot \left(h_{air,in} - h_{air,out}\right)
\end{aligned} \tag{32}
$$

The mass transfer coefficient can be calculated by Equation 33 and the necessary fluid properties by Equations 34-37 (Heyns, 2008):

$$h_d = \frac{5.5439/10^8 {Re_{wm}}^{0.15} {Re_{awm}}^{0.9}}{{d_o}^{1.6}} \tag{33}$$

$$Nu_c = \frac{\alpha_c d_i}{k_c} = 0.023 * {Re_c}^{0.8} {Pr_c}^{0.4}\left(0.55 + 2.09\left(\frac{p_{crit}}{p_{vap}}\right)^{0.38}\right) \tag{34}$$

$$Re_{awm} = \frac{\rho_{avm} \cdot v_{avm} \cdot d_o}{\mu_{wm}} \; where \; v_{avm} = \frac{m_{air}}{\rho_{avm} A_{air}} \tag{35}$$

$$Re_{wm} = \frac{4\Gamma_m}{\mu_{wm}} \tag{36}$$

$$\Gamma_m = \frac{m_w \cdot d_o}{A_{bundles}} \tag{37}$$

The air outlet enthalpy is calculated by Equation 38:

$$h_{air,out} = h_{air,avm} - (h_{air,avm} - h_{air,in})e^{\frac{A_{bundles} h_d}{m_{air}}} \tag{38}$$

The condensation heat transfer coefficient is given by Equations 40 for $Re_{ss} < 35000$. Equation 41 is used for Reynolds numbers higher than 35000. The Reynolds number is given by Equation 39 (Bergman et al., 2006):

$$Re_{cv} = \frac{\rho_{cv} \cdot v_{cv} \cdot d_i}{\mu_{cv}} \; and \; Re_{cl} = \frac{\rho_{cl} \cdot v_{cl} \cdot d_i}{\mu_{cl}} \tag{39}$$

$$\alpha_c = \frac{\left[\frac{0.555((g\rho_{cl}(\rho_{cl} - \rho_{cv})(h_{vap} + 0.68 * cp_{cl}(T_c - T_{wall}))d_i{}^3}{\mu_{cl} k_{cl}(T_c - T_{wall})}\right]^{1/4}}{d_i} k_{cl} \tag{40}$$

$$\alpha_c = \frac{0.023 {Re_{cl}}^{0.4} {Pr_{cl}}^{0.8}(0.55 + \left(\frac{p_{crit}}{p_{cv}}\right)^{0.38}}{d_i} k_{cl} \tag{41}$$

The deluge water heat transfer coefficient and the tube wall overall heat transfer coefficient are given by Equations 42-43:

$$\alpha_w = 2102.9\left(\frac{\Gamma_m}{d_o}\right)^{0.333} \tag{42}$$

$$U = \frac{1}{\left(\frac{1}{\alpha_w} + \frac{d_o}{d_i k_{pipe}} + \frac{1}{\alpha_c}\right)} \tag{43}$$

One of the main questions was quantity of the evaporated water, which is given by Equation 44:

$$m_{water} = m_{air}(w_{air,\,out} - w_{air,in}) \tag{44}$$

In dry mode, the mass transfer doesn´t take place, the air absorbs the rejected heat by condensation. The important parameters in this case are described by Equations 45-47 (Bergman et al., 2006):

$$\begin{aligned} Q_{cond} = m_{R245fa} \cdot (\Delta L_{cond} + \Delta h_{R245fa,cool}) = Q_{heat\ transfer} \\ = UA\left(T_c - T_{air,avg}\right) = Q_{heat+mass\ transfer\ (air\ side)} \\ = m_{air} \cdot \left(h_{air,in} - h_{air,out}\right) \end{aligned} \tag{45}$$

$$\begin{aligned} \alpha_{a,dry} = \left(0.3 + \frac{0.62 Re_{air,wall}{}^{0.5} Pr_{air,wall}{}^{\frac{1}{3}}}{\left(1 + \left(\frac{0.4}{Pr_{air,wall}}\right)^{\frac{2}{3}}\right)^{0.25}}\right)\Bigg(1 \\ + \left(\frac{Re_{air,wall}}{282000}\right)^{\frac{5}{8}}\Bigg)^{4/5} \frac{k_{air,wall}}{d_o} \end{aligned} \tag{46}$$

$$U = \frac{1}{\left(\frac{1}{\alpha_{a,dry}} + \frac{d_o}{d_i k_{pipe}} + \frac{1}{\alpha_c}\right)} \tag{47}$$

In the calculation, many parameters are unknown, like the mean deluge water temperature, or the condensation temperature (as it changes by the inlet air temperature) and the air average temperature, where Re_{awm} was evaluated, the air outlet temperature and the wall temperature. The wall temperature doesn´t really change the coefficient, which is related to it, but the other parameters have a crucial role. To find the condensation temperature for a given air temperature, a nested loop iteration was used, with the deluge water temperature and the condensation temperature changed in the iteration.

The given data of the condenser didn´t contain the exact geometric parameters of the evaporative condenser, like number of tubes, just one tube diameter. To overstep this problem, a surface was suggested, which can fulfil the criterion to use the condenser at 22°C when the design outlet temperature is 11.2°C, as was suggested by Mannvit. When choosing the surface size, it was also considered, that during winter it must work in a dry mode, as the water could freeze in the tubes and destroy them. This would reduce the efficiency of the plant very much, as the overall heat transfer coefficient can be two orders of magnitude less if on one side there is gas instead of liquid. The mass flow of the ORC fluid was also unknown, but Mannvit Consulting Engineers provided official data on the power output of the two screw expanders in the plant, and the geothermal fluid inlet and outlet temperatures and pressures in many points. To determine the mass, a flow reverse calculation was used, where the following parameters were fixed:

- The design condensation temperature;
- The geothermal water mass flow temperature and pressure values in most of the brines.

During the calculation the pressure drop on the ORC side was neglected, the turbine isentropic efficiency was estimated based on typical values found on-line (Hsu et al., 2014).

The ORC high-temperature loop was calculated with the following routines, based on the schematic drawing of the power plant (Appendix I). The red marks show the known parameters, while the blue circles show states with unknown parameters. In the high-temperature loop in the evaporator the geothermal water goes with full capacity and evaporates and slightly superheats the ORC fluid as defined in Equation 48:

$$m_{g1}(h_{g1} - h_{g2}) = m_{r245fa}(h_3 - h_{4SH}) \tag{48}$$

After the evaporator, a bigger portion of the geothermal water goes to the low-temperature loop, and a smaller fraction preheats the ORC fluid (Equation 49):

$$m_{g2}(h_{g2} - h_{g3}) = m_{r245fa}(h_2 - h_3) \tag{49}$$

The expander work's is given by Equation 50, with the screw expander power output known (W_0):

$$W_t = m_{r245fa}(h_{4SH} - h_5) \tag{50}$$

6. RESULTS OF THE EVAPORATIVE CONDENSER SIMULATION

The pump work was assumed to be isentropic (this assumption doesn´t make significant change in the temperature of point 2), $s_1=s_2$. With numbers of points referring to the figure in Appendix I, the ORC fluid pressure at 2, 3, 4 and 4SH points was set to be the same, temperature at 3 and 4 is the same, while the temperature difference between the superheated vapour and the evaporated vapour was assumed to be 2°C. By iterating with the mass flow, the optimal pressure was found by an iterative method, which gave the right pressure, which results in the known power output ($W_t=W_0$). By plotting the temperatures of the geothermal fluid and the ORC fluid versus the ORC mass flow, and also represent the known geothermal temperatures (T_{g2}=104°C, T_{g3*}=78°C, and T_{g3}= T_{g4*} =38°C, respectively), the cross point of the mass flow dependent geothermal fluid temperature and the designed geothermal fluid temperature gives the possible ORC mass flow. The two known geothermal temperatures in a precise calculation would cross the calculated geothermal temperatures at the same mass flow, but as any losses etc. at the evaporator and preheater were not taken into account, it could result in some difference, adding also that the expander efficiency has great effect on the results. The stronger boundary is the higher fixed geothermal temperature, as it has to be an evaporative medium in the low-temperature loop. As can be seen, the temperature difference between the calculated geothermal water temperature at (T_{g3}) and the reference temperature is not crucial. This was also done for the low-temperature loop. The reverse calculations resulted in 52 and 43 kg/s mass flow for the high- and low-temperature loops, respectively, and 11.9 and 6.46 bar inlet pressure to the expander. With the known mass flow, temperature and pressure values, the behaviour of the evaporative condenser was modelled.

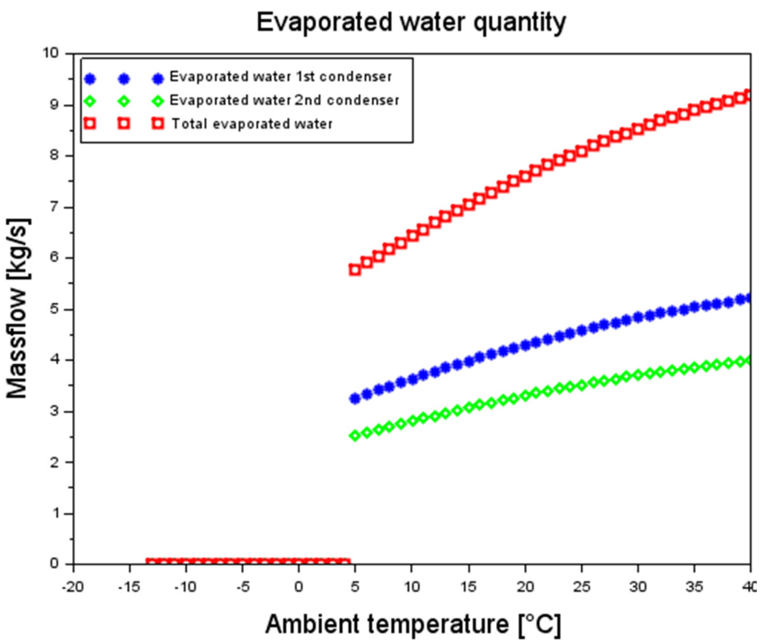

FIGURE 9: Evaporated water mass flow vs ambient temperature

As seen in Figure 9, the model shows that the evaporated water mass flow is around 8-9 kg/s. It is influenced mostly by the heat exchanger surface area and the air mass flow. As the air temperature increases, the air can carry more water vapour. Therefore, higher temperature will result in a higher water evaporation rate. The condenser temperature will also rise, as it physically cannot be lower than the air inlet wet bulb temperature. It will raise the condenser pressure and reduce the power plant efficiency as presented in Figures 10 and 11. In the dry mode, the efficiency will also be reduced, as the overall heat transfer coefficient is controlled by the air side conduction heat transfer coefficient, which is two magnitudes lower than water conduction heat transfer coefficient. The temperature duration curve and the related

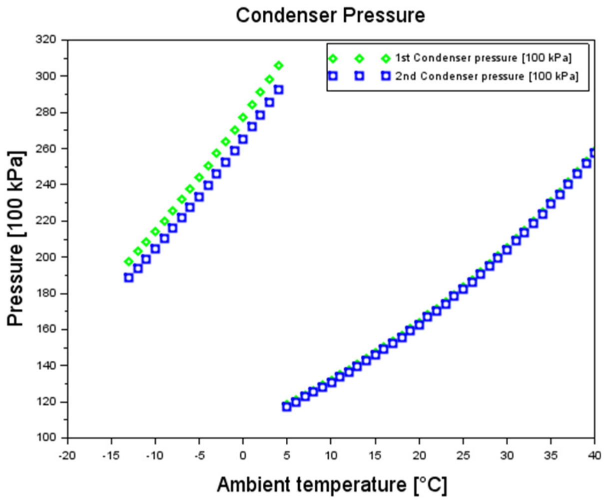

FIGURE 10: Condenser pressure vs ambient temperature

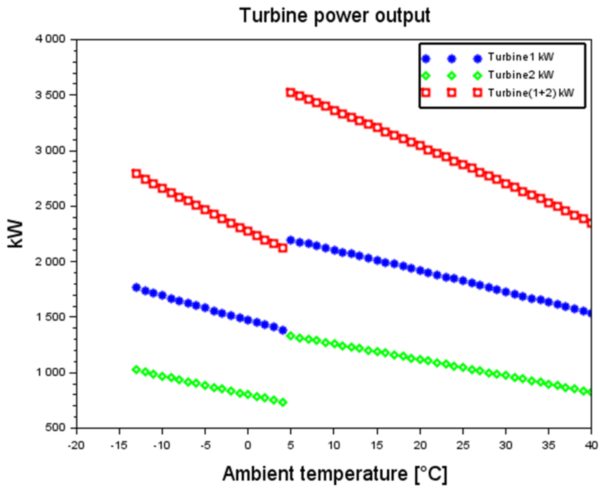

FIGURE 11: Turbine power output curve vs ambient temperature

performance duration curve can be seen in Figure 12. The power plant will work close to the design power output most of the time.

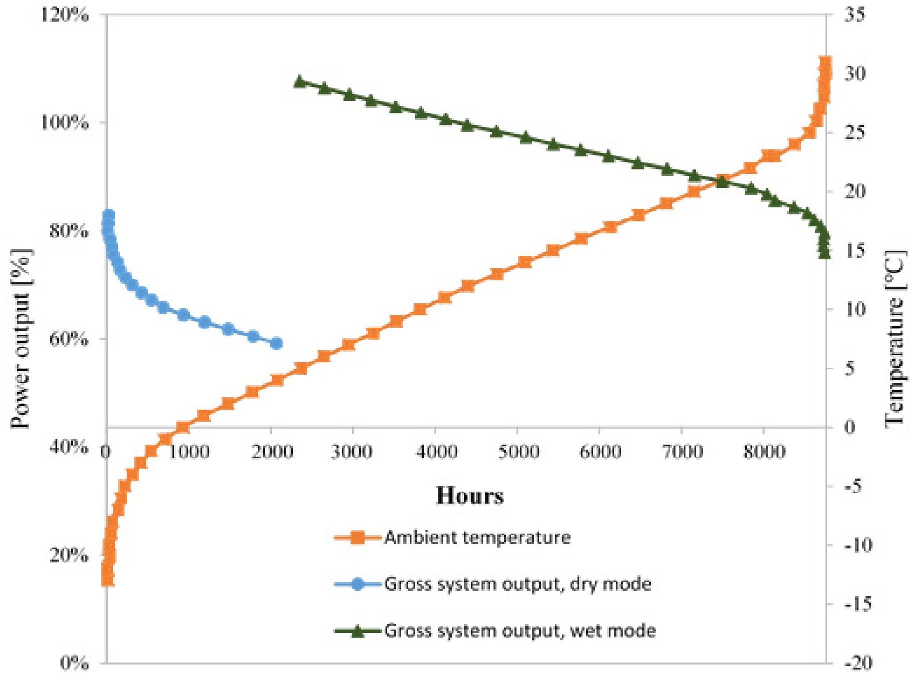

FIGURE 12: Temperature and power output duration curve

7. CONCLUSIONS

The project was conducted to find the possible heat that the ORC power plant in Tura can supply to a planned greenhouse complex and investigate the behaviour of the evaporative condenser. Scilab dynamic simulations were used to determine the heat requirements of the greenhouses and a static model was designed to evaluate the evaporative condenser behaviour and the effect on the turbine output. The calculated income is between 574 000 and 805 000 EUR per year. The evaporated water quantity varies greatly by the ambient temperature as well as the turbine power output.

The simulation of the greenhouse could be supplemented if the transpiration heat loss of the plants was more accurately calculated, and with a smoother temperature data.

The lack of power plant data resulted in many assumptions in the evaluation of the evaporative condenser. With more precise data, the calculations could be refined and give a more accurate result. But as it the case for every model, it needs validation with real measurements.

The calculated low power output for the dry operation of the evaporative condenser at low air temperatures is highly interesting. Either elimination of the dry mode by a condenser design which can tolerate some freezing on the outside of the tubes has to be made, or a way found to have fins on the tube outside to enhance the performance in the dry mode.

ACKNOWLEDGEMENTS

I would like to thank the UNU-GTP for granting me the opportunity to participate in the six-month training program. Special thanks to the director Mr. Lúdvík S. Georgsson, his deputy Mr. Ingimar G. Haraldsson, Ms. Thórhildur Ísberg, Mr. Markús A. G. Wilde and Ms. Málfríður Ómarsdóttir and every teacher who was involved in the training.

I would like to express my gratitude to Páll Valdimarsson for being my supervisor and Kristinn Ingason at Mannvit Consulting Engineers for the help and the project. I would also like to say thanks for help and professional assistance to Nasim Saber, her friend Argineh Shabandari and Gideon Gitonga Gitobu.

I would also like to thank all the students that made this time wonderful, special thanks to Zsófi Erzsébet Unyi, Byron Fabian Pilicita Masabanda, Sarantseteseg Lkhagvasuren. the whole geothermal utilisation group: Gideon Gitonga Gitobu, Nasim Saber, Winnie Adhiambo Apiyo, Daniel Wanga Odongo, Harrison Kiplimo Keter, and Zoltán Békés.

And last but not least thanks to my family and friends, who supported me the whole year, not least during my time in Iceland!

REFERENCES

Alternatív Energia, 2016: *Vegetables produced by thermal water in Tura (in Hungarian)*. Alternativ Energia, website: *www.alternativenergia.hu/termalvizzel-termelnek-zoldseget-turan/76093*

Anon, 1977: *DIN 4703 Teil 3. Varmeleistung von Raumheizkörper* (in German). Beuth Verlag, Berlin, Germany.

Bergman, T.L., Lavine, A.S., Incropera, F.P., and DeWitt, D.P., 2006: *Introduction to heat transfer* (6th ed.). John Wiley & Sons, NY, 912 pp.

CoolProp 2016: *CoolProp C++ library*. CoolProp*, website: www.coolprop.org*.

Duffie, J.A., and Beckman, W.A., 2013: *Solar engineering of thermal processes* (4th edition). John Wiley & Sons, New Jersey, 928 pp.

EnergyPlus, 2016: *Weather data*. EnergyPlus, website: *energyplus.net/weather.*

Fögáz, 2016: *Present heat prices. FŐGÁZ,* website:
www.fogaz.hu/Egyetemes-Szolgaltatas/Ugyintezes/Arak-dijszabasok/Aktualis-arak?download

Google Earth, 2016: *Google Earth software.* Google Earth, website: *www.google.com/earth*
Heyns, J.A., 2008: *Performance characteristic of an air-cooled steam condenser incorporating a hybrid (dry/wet) dephlegmator*. University of Stellenbosch, S-Africa, MSc thesis, 129 pp.

Hsu, S.-W., Chiang H.-W.D., and Yen, C.-W., 2014: Experimental investigation of the performance of a hermetic screw-expander Organic Rankine Cycle. *Energies 2014, 7,* 6172-6185.

Hungarian Ministry of National Development, 2011: *Regulation about the support of district heating, "51/2011, (IX. 30.).* NFM, website: *net.jogtar.hu.*

Kröger, D.G., 2004: *Air cooled heat exchangers and cooling towers* (vol. 1). PennWell Corp. Tulsa, OK, 502 pp.

Magyar Idők, 2016: *Ten billion investment to utilise the thermal water in Tura* (in Hu.). Magyar Idök, website: *magyaridok.hu/gazdasag/tizmilliardos-beruhazas-turai-termalviz-hasznositasara-691921*

Mariani, L., Cola, G., Bulgari, R., Ferrante, and Martinetti, L., 2016: Space and time variability of heating requirements for greenhouse tomato production in the Euro-Mediterranean area. *Science of the Total Environment, 562,* 834-844.

MATLAB, 2016: *MATLAB, the language of technical computing*. MATLAB, *website: se.mathworks.com.*

OECD, 2015: *Projected costs of generating electricity.* Nuclear Energy Agency, OECD, website: www.oecd-nea.org/ndd/pubs/2015/7279-proj-costs-electricity-2015-es.pdf.

Rafferty, K.D., 1998: Greenhouses. In: Lienau, P.J., and Lunis, B.C. (eds.), *Geothermal direct use engineering and design guidebook.* Geo-Heat Center, Klamath Falls, OR, 307-326.

REFPROP, 2016: *NIST Reference fluid thermodynamic and transport properties database (REFPROP), version 9.1*. National Institute of Standards and Technology – NIST, website: *www.nist.gov/srd/refprop.*

Sanford, S., 2011: *Using curtains to reduce greenhouse heating and cooling costs*. Energy Efficiency in Greenhouses, article, 8 pp, website: *articles.extension.org/sites/default/files/4.%20A3907-03.pdf.*

Scilab, 2016: *Scilab 5.5.2*. Scilab Enterprises, website*: www.scilab.org.*

Tura Organic Garden, 2015: *Decisions*. Middle-Danube-Valley Inspectorate for Environmental Protection, Nature Conservation and Water Management, website:
kdvktf.zoldhatosag.hu/dokumentumok/hirek/5114/4425/34020_20_2014.pdf

Unyi, Z.E., 2016: Geothermal reservoir model of Dombovar area, SW-Hungary. Report 40 in: *Geothermal training in Iceland 2016.* UNU-GTP, Iceland, 875-890.

Zelzouli, K., Guizani, A., Sebai, R., and Kerkeni, C., 2012: Solar thermal systems performances versus flat plate solar collectors connected in series. *Engineering, 4-12,* 881-893.

NOMENCLATURE

Symbol	Description	Unit
A	Surface	m^2
A_{roof}	Surface of the greenhouse roof	m^2
$A_{bundles}$	Surface of the tube bundles in the condenser	m^2
A_{air}	Surface where the air can pass in the condenser	m^2
α	Convective heat transfer coefficient	$W/(m^2K)$
α_a	Conductive heat transfer coefficient of air	$W/(m^2K)$
$\alpha_{a,dry}$	Conductive heat transfer coefficient of air	$W/(m^2K)$
α_c	Conductive heat transfer coefficient of ORC medium	$W/(m^2K)$
α_w	Conductive heat transfer coefficient of water	$W/(m^2K)$
β	Angle between the horizon and the surface	°
C	Opaque sky factor	
CF	Constant	
c_p	Specific heat	J/(kgK) or J/(kg°C)
cp_{cl}	Heat capacity of ORC condensate	J/(kgK) or J/(kg°C)
δ	Thickness or Stefan Boltzmann constant	m or $W/(m^2K)$
ΔTlg	Logarithmic mean temperature difference	°C
ΔTlg_0	Logarithmic mean temperature difference design condition	°C
ΔTlg_{HX}	Logarithmic mean temperature difference in the heat exchanger	°C
ΔL_{cond}	Latent heat of vaporization	J/kg
$\Delta h_{R245fa,cool}$	Specific enthalpy change of ORC fluid during cooling	J/kg
d_i	Inlet diameter	m
d_o	Outer diameter	m
ε_{glass}	Emissivity of the glass	
ε_{sky}	Emissivity of the sky	
F	View factor	
g	Gravity	m/s^2
φ	Latitude of the place in degrees	°
Γ_m	Deluge water mass flow per unit length	kg/(m s)
γ	Surface azimuth angle	°
h_d	Mass transfer coefficient	$kg/(sm^2)$
h_v	Specific enthalpy of vapour	J/kg
h_{air}	Specific enthalpy of air	J/kg
$h_{air,avm}$	Specific enthalpy of air at mean water temperature	J/kg
h_{vap}	Specific enthalpy of vaporisation of water	J/kg
h_{g1}, h_{g2}	Specific enthalpy of the geothermal fluid in different points	J/kg
	Specific enthalpy of superheated ORC fluid	J/kg
h_3, h_5, h_{4SH}	Specific enthalpy of ORC fluid in different points	J/kg
I_{direct}	Direct radiation	W/m^2
$I_{diffuse,sky}$	Diffuse radiation from the sky	W/m^2
$I_{diffuse,ground}$	Diffuse radiation from the ground	W/m^2
I_{global}	Global radiation	W/m^2
I_{diff}	Diffuse radiation	W/m^2
I_s	Sum of radiation	W/m^2
k_{cl}	Thermal conductivity of the condensate	W/(mK)
k_{pipe}	Thermal conductivity y of pipe material	W/(mK)
$k_{air,wall}$	Thermal conductivity of air at the bundle´s wall temperature	W/(mK)
λ	Conductive heat transfer coefficient	W/(mK)
m_{rad}	Mass flow in the radiator	kg/s
m_g	Mass flow of geothermal fluid	kg/s
m_w	Mass flow of deluge water	kg/s
m_{air}	Mass flow of air	kg/s
m_{R245fa}	Mass flow of ORC fluid	kg/s

Symbol	Description	Unit
m_{water}	Mass flow of evaporated water	kg/s
μ_{wm}	Dynamic viscosity	N s/m^2
μ_{cv}	Dynamic viscosity of the condensing ORC vapour	N s/m^2
μ_{cl}	Dynamic viscosity of the condensed ORC liquid	N s/m^2
Nu_c	Nusselt number	
n	Air exchange rate, or number of the day in a year sequence	1/s or 1/h
Pr_c	Prandtl number	
Pr_{ws}	Prandtl number	
$Pr_{air,wall}$	Prandtl number	
p_{crit}	Critical pressure	Pa
p_{cv}	Vapour pressure	Pa
Q_{sr}	Heat gain rate by solar radiation	W, MW
Q_{add}	Heat supply rate by the greenhouse heating system	W, MW
Q_f	Heat loss by rate filtration	W, MW
Q_t	Heat loss by rate transmission	W, MW
Q_r	Heat loss rate by radiation	W, MW
Q_{GH}	Heat power requirement of the greenhouse	W
$Q_{0,GH}$	Heat power requirement of the greenhouse design cond.	W
Q_{HX}	Heat power supply by the geothermal heat exchanger	W
$Q_{heat+mass\ transfer}$	Sum of heat and mass transfer rate	W
$Q_{heat\ transfer}$	Heat transfer rate between deluge water and condensate	W
Q_{cond}	Heat rate of cooling and condensing of ORC fluid	W
Re_{awm}	Reynolds number of air at mean water temperature	
r	Reflectance	
Re_{wm}	Reynolds number of mean water	
Re_c	Reynolds number of condensate	
Re_{cv}	Reynolds number of condensing vapour	
$Re_{air,wall}$	Reynolds number of air at wall temperature	
ρ_{cv}	Density of ORC vapour	kg/m^3
ρ_{avm}	Density of air at mean water temperature	kg/m^3
ρ_{cl}	Density of ORC condensate	kg/m^3
ρ_{air}	Density of air at ambient temperature	kg/m^3
T	Temperature	K
$T_{roof,out}$	Temperature of the roof	°C
T_{sky}	Temperature of the sky	°C
T_{amb}	Ambient temperature	°C
$T_{air,dew}$	Dew temperature of the ambient air	°C
$T_{g,in}$	Temperature of geothermal fluid at the inlet	°C
$T_{rad,x}$	Temperature of radiator fluid after the heat exchanger	°C
$T_{g,out}$	Temperature of geothermal fluid at the outlet	°C
$T_{rad,return}$	Temperature of radiator coming from the greenhouse	°C
T_w	Temperature of water	°C
T_a	Temperature of air	°C
T_c	Temperature of condensate	°C
T_{wm}	Mean water temperature	°C
T_{wall}	Temperature of the wall	°C
$T_{air,avg}$	Average air temperature	°C
θ	Angle of incidence	°
θ_z	Zenith angle	°
U	Overall heat transfer coefficient	W/(m^{2}K)
v_{wind}	Wind velocity	m/s
V	Volume of air in the greenhouse	m^3
w	Absolute humidity	g/kg air
w_{ws}	Absolute humidity at water surface	g/kg air
v_{avm}	Velocity of air at the water surface	m/s
v_{cv}	Velocity of the condensing ORC vapour	m/s

Symbol	Description	Unit
v_{cl}	Velocity of the condensed ORC liquid	m/s
w_{air}	Absolute humidity of air	g/kg air
W_t	Power output of turbine	W

APPENDIX I: Schematic design of Tura ORC power plant